Dalton Transactions

Accepted Manuscript

This is an *Accepted Manuscript*, which has been through the Royal Society of Chemistry peer review process and has been accepted for publication.

Accepted Manuscripts are published online shortly after acceptance, before technical editing, formatting and proof reading. Using this free service, authors can make their results available to the community, in citable form, before we publish the edited article. We will replace this *Accepted Manuscript* with the edited and formatted *Advance Article* as soon as it is available.

You can find more information about *Accepted Manuscripts* in the Information for Authors.

Please note that technical editing may introduce minor changes to the text and/or graphics, which may alter content. The journal's standard Terms & Conditions and the Ethical guidelines still apply. In no event shall the Royal Society of Chemistry be held responsible for any errors or omissions in this *Accepted Manuscript* or any consequences arising from the use of any information it contains.

ROYAL SOCIETY OF CHEMISTRY

www.rsc.org/dalton

Graphic Abstract:

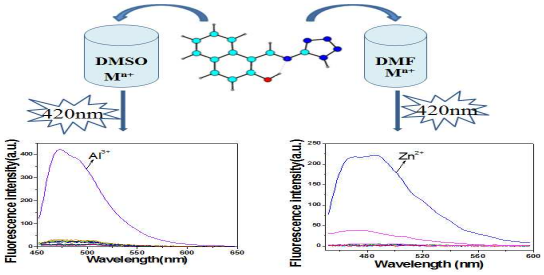

A dual fluorescent chemosensor for Al^{3+} and Zn^{2+} ions based on inhibition of ESIPT can be applied in bioimaging .

Dalton Transactions Accepted Manuscript

Journal Name

RSCPublishing

ARTICLE

A Tetrazole-based Fluorescence "Turn-On" Sensor for Al(III), Zn(II) ions and Its Application in Bioimaging

Cite this: DOI: 10.1039/xoxxoooooox

Received ooth January 2012,
Accepted ooth January 2012

DOI: 10.1039/xoxxoooooox

www.rsc.org/

Wei-Hua Ding, Wei Cao, Xiang-Jun Zheng,* Wan-Jian Ding,* Jin-Ping Qiao, Lin-Pei Jin

A Tetrazole derivative 1-[(1H-tetrazol-5-ylimino)methyl]naphthalen-2-ol (H_2L) as fluorescent chemosensor for Al^{3+} in DMSO and Zn^{2+} in DMF was designed and synthesized. From ^{1}HNMR data, Job plot and ESI-MS spectrum, 1:1 stoichiometric complexation between H_2L and Al^{3+}/Zn^{2+} was found in DMSO and DMF, respectively. The theoretical calculations at the level of B3LYP/6-311G** for ground state and TD-B3LYP/6-311G** for excited state revealed the sensing mechanism is the inhibition of excited state intramolecular proton transfer (ESIPT). And the possible fluorescent species formed in the DMSO and DMF solutions were deduced to be [Al(HL)(OH)(NO_3)(H_2O)(DMSO)] and [Zn(HL)(OH)(H_2O)(DMF)]. What's more, It is confirmed that H_2L could be used to detect Al^{3+} and Zn^{2+} in cells by bioimaging.

Introduction

In recent years, the development of fluorescent chemosensors toward biologically and environmentally important species has attracted increasing attention for their high sensitivity, simplicity and real-time monitoring with rapid response time.[1] Aluminum, the most prevalent metal element in the earth's crust, is widely used in modern life with a variety of applications.[2,3] However, high amounts of aluminum ion in human body may lead to some health issues, for instance, Parkinson's disease, dialysis encephalopathy, impairment of memory and osteoporosis.[4,5] Zinc, the second most abundant transition metal ion in the human body, plays an important role as an anti-oxidant.[6,7] Besides, Zn^{2+} is actively involved in diverse fundamental biological processes, such as structural and catalytic cofactors, gene transcription, regulation of metalloenzymes, neural signal transmission and apoptosis.[8-11] A small quantity of Zn^{2+} is necessary for the living organism, while extremely high intakes will bring in some overt toxicity symptoms and neurodegenerative disorders.[12-16] Owing to the importance of Al^{3+} and Zn^{2+}, many fluorescent sensors for separate detection of Al^{3+} ion[17-25] and Zn^{2+} ion[26-37] have been reported. However, most of them contain potential toxic substance in their ingredients, which will pollute the environment and do harm to human health. In addition, many sensors require complicated syntheses involving harsh reaction conditions and expensive chemicals. More importantly, very few fluorescent chemosensors can selectively detect both Al^{3+} and Zn^{2+} simultaneously.[38,39] It is desirable to develop fluorescent chemosensors with high selectivity and sensitivity for multi-metal ions that are easily prepared and can be applied in vivo and in vitro. This is a real challenge.

Tetrazole derivatives have received special attention due to its wide applications in medicinal chemistry and pharmacology,[40-43] materials chemistry,[44] organometallic and coordination chemistry,[45,46] and organocatalysis.[47-49] Compounds containing tetrazole rings have particular biological activities, which are usually attributed to the possibility of this moiety to mimic a carboxyl group or a *cis*-amide bond.[50] It is reported that many drugs containing this fragment have been used in various branches of medicine. Those suggest that some tetrazole derivatives have a low toxicity to environment and human body. In addition, chemosensors containing nitrogen- and oxygen-rich coordination atoms generally bind multi-metal ions depending on reaction conditions.[51-54] Herein, we report a tetrazole derivative (H_2L) as the fluorescence "turn-on" chemosensor for distinct detections of Al^{3+} and Zn^{2+} based on inhibited excited-state intramolecular proton transfer (ESIPT). The ESIPT mechanism was inferred through experimental and DFT theoretical methods. Furthermore, the chemosensor was used to detect the Al^{3+} and Zn^{2+} ions in cells by bioimaging.

Results and Discussion

Fluorescent response of H_2L to metal ions in different solvent

Dalton Transactions Accepted Manuscript

H_2L was soluble in DMSO and DMF, slightly soluble in CH_2Cl_2 and insoluble in water and alcohols. The selectivities of H_2L to various metal ions were examined in DMSO and DMF. The addition of 1.0 equiv of Na^+, K^+, Mg^{2+}, Ca^{2+}, Mn^{2+}, Fe^{3+}, Co^{2+}, Cr^{3+}, Cd^{2+}, Cu^{2+}, Pb^{2+}, Ni^{2+}, Zn^{2+} and Al^{3+} ions was used to measure the selectivity of H_2L for metal ions in DMSO and DMF, respectively. As shown in Fig. 1a, H_2L itself displays very weak fluorescence emission in DMSO and only Al^{3+} ion causes a large fluorescence intensity enhancement at 470 nm, while no obvious fluorescent response could be observed upon the addition of other metal ions. However, in the DMF solution of H_2L, Zn^{2+} caused a significant fluorescence enhancement at 483 nm, and Al^{3+} displayed a weak fluorescence enhancement, while other metal ions have no effect on the fluorescence emission (Fig. 1b).

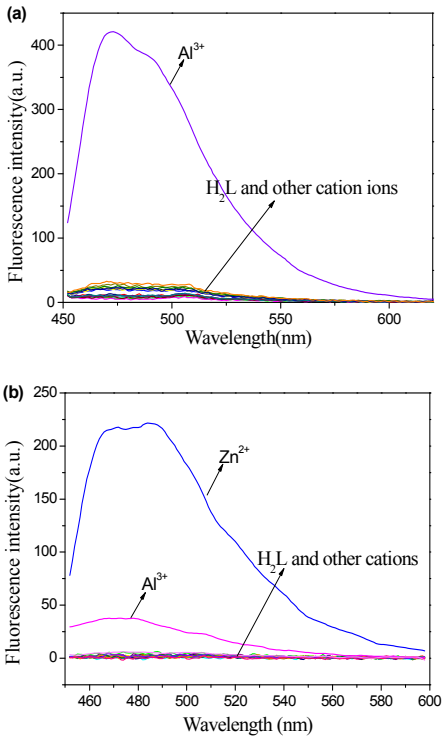

Fig. 1 (a) Fluorescence responses of H_2L (20 μM) in DMSO with 1.0 equiv of Al^{3+}, Zn^{2+}, Cd^{2+}, Co^{2+}, Ca^{2+}, Cr^{3+}, Mn^{2+}, Ni^{2+}, Fe^{3+}, Cu^{2+}, Pb^{2+}, Na^+, K^+ and Mg^{2+}. λ_{ex} = 420 nm. (b) Fluorescence responses of H_2L (20 μM) in DMF with 1.0 equiv of above metal ions. λ_{ex} = 420 nm.

To validate the high selectivity of H_2L as a chemosensor for the detection of Al^{3+} and Zn^{2+} in practice, the competitive experiments were carried out by addition of 1.0 equiv of Al^{3+}/ Zn^{2+} to the H_2L solutions in the presence of 1.0 equiv of other metal ions. As shown in Fig. S1a, there is no interference for the detection of Al^{3+} in presence of other metal ions. Furthermore, Zn^{2+} can be easily detected in the presence of some competing metal ions (Fig. S1b). These results demonstrate that H_2L displays an excellent selectivity for Al^{3+} in DMSO solution and H_2L has higher selectivity for Al^{3+} than Zn^{2+}.

Stoichiometric complexation and association constants of H_2L with Al^{3+} and Zn^{2+} and their detection limits

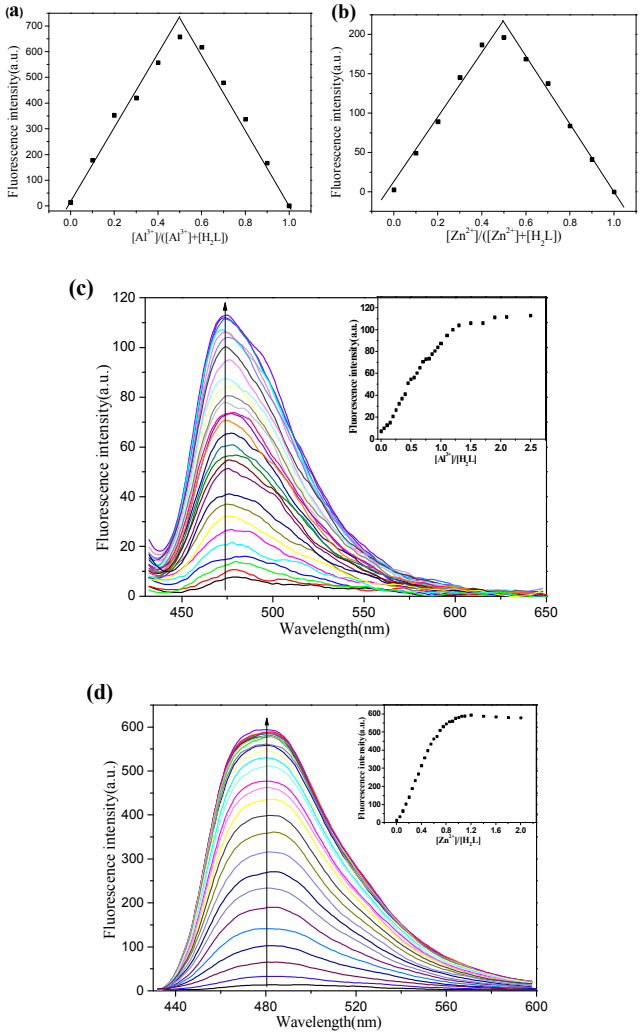

Fig. 2 Job plot for the determination of the stoichiometry in the complexation of H_2L with Al^{3+} in DMSO (a), H_2L with Zn^{2+} in DMF (b); Fluorescence titration profiles (λ_{ex} = 420 nm) of H_2L in the presence of increasing amounts of Al^{3+} in DMSO, inset: the emission intensity of H_2L with the Al^{3+} increasing at 470nm (c), and of Zn^{2+} in DMF, inset: the emission intensity of H_2L with the Zn^{2+} increasing at 483nm (d).

The Job plot was obtained from emission data. As shown in Fig. 2a and b, 1:1 stoichiometric complexation of H_2L with Al^{3+} in DMSO and Zn^{2+} in DMF was confirmed. In the fluorescence titration profiles (Fig. 2c and 2d), an increase of fluorescence intensity could be observed with increasing Al^{3+} and Zn^{2+} concentration until 1.0 equiv, while the emission intensity tends to be the same with further increase of Al^{3+} and Zn^{2+} concentration. The saturation behaviors of the fluorescence intensity after 1.0 equiv of Al^{3+} and Zn^{2+} also reveal the 1:1 stoichiometry

Based on the fluorescence titration data, the association constant K of complexation of H_2L with Al^{3+} and Zn^{2+} was

Dalton Transactions Accepted Manuscript

This journal is © The Royal Society of Chemistry 2012

calculated by the Benesi-Hildebrand expression.[55] The association constants were determined to be 1.02×10^4 for the complex of H_2L with Al^{3+} in DMSO and 5.06×10^4 for the complex of H_2L with Zn^{2+} in DMF (Fig. 3a and 3b). Besides, in Fig. 3c and 3d, a linear regression curve was obtained between the maximum fluorescence intensity and the minimum fluorescence intensity, and the detection limit of H_2L for Al^{3+} was 5.86×10^{-6} mol·L^{-1} in DMSO and for Zn^{2+} was 1.81×10^{-6} mol·L^{-1} in DMF.[55] The results of the detection limits for Al^{3+} and Zn^{2+} ions are comparable with the reported.[21, 27, 56, 57] These results also proved the high sensitivity of H_2L towards Al^{3+} in DMSO and Zn^{2+} in DMF.

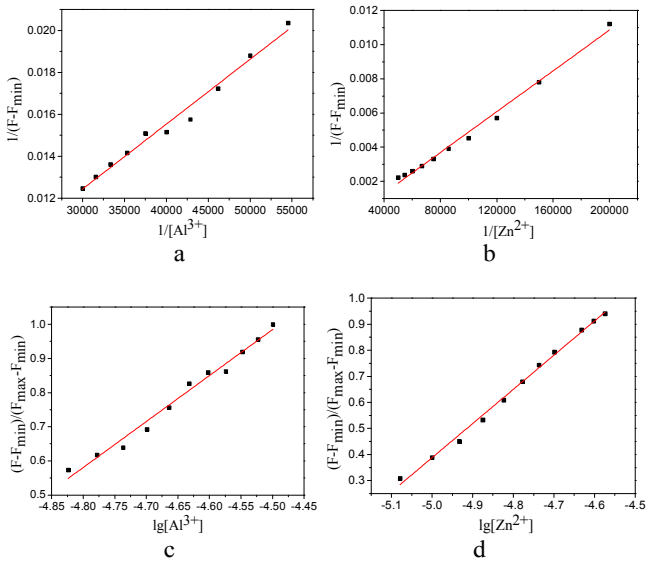

Fig. 3 Benesi-Hildebrand plot of H_2L with Al^{3+} in DMSO(λ_{em} = 470 nm) (a), and with Zn^{2+} in DMF(λ_{em} = 483 nm) (b); Normalized response of emission signal changing Al^{3+} concentrations at 470nm (c) and changing Zn^{2+} concentrations at 483 nm (d).

Binding modes of H_2L for Al^{3+} and Zn^{2+}, and possible fluorescent species formed in the solution

The binding modes of H_2L for Al^{3+} and Zn^{2+} were further confirmed by ^{1}HNMR titration experiments. First, the assignment for H_2L in DMSO-d_6 and in DMF-d_7 was established by ^{1}HMBC, ^{1}HSQC, and H-H COSY (Fig. S2 and S3). The binding mode of H_2L with Al^{3+} was examined in DMSO-d_6, as shown in Figure 4a. Upon complexation with Al^{3+} ions, the proton signal of the naphthol hydroxyl at 13.34 ppm disappeared. The proton peak (H_7) of CH=N downfield shifted from 10.11 ppm to 10.80 ppm. Similarly, upon complexation with Zn^{2+} ions in DMF-d_7, the naphthol hydroxyl at 14.12 ppm also disappeared and the proton peak of CH=N downfield shifted from 10.50 ppm to 10.95 ppm (Fig. 4b). The other aromatic protons showed a slight change for the both systems. The results suggest that Al^{3+} and Zn^{2+} are coordinated with the imine nitrogen atom and the hydroxyl oxygen atom of H_2L. In addition, there were no significant changes with the proton peaks upon the addition of 1.5 equiv of Al^{3+} or Zn^{2+} to H_2L. This also confirms the 1:1 stoichiometry for H_2L to Al^{3+} or Zn^{2+}. From Fig. 4(a) (II) and (III) we can see new signals at 11.98 ppm and 6.45 ppm appeared, while the signals disappeared when drops of D_2O were added (Fig. 4(a)(□)). These active hydrogen signals indicate hydroxyl- and water-containing species formed. This could be realized that even hydrated Al(III) salts may suffice to hydrolyze and form hydrated Al(III) compounds.[58] The similar phenomenon appeared in Fig. 4(b).

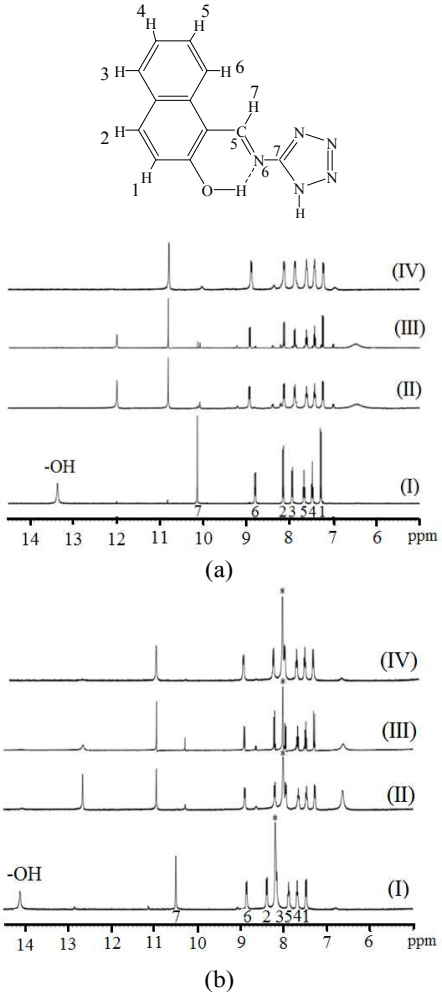

Fig. 4 ^{1}HNMR spectra (a) in DMSO-d_6: (I) H_2L, (II) H_2L+1.0 equiv of Al^{3+}, (III) H_2L+1.5 equiv of Al^{3+}, (IV) H_2L+1.0 equiv of Al^{3+}+D_2O; (b) in DMF-d_7: (I) H_2L, (II) H_2L+1.0 equiv of Zn^{2+}, (III) H_2L+1.5 equiv of Zn^{2+}, (IV) H_2L+1.0 equiv of Zn^{2+}+D_2O, the DMF-d_7 peak at 8.1943 ppm is labelled with asterisks*.

To further study the coordination of H_2L with Al^{3+} and Zn^{2+}, their ESI mass spectra were carried out. As shown in Fig. 5a, the mass spectrum of H_2L upon addition of 1.0 equiv of Al^{3+} exhibited an intense peak at m/z 385.0037 and a weak one at m/z 463.1079, corresponding to the ion $Na^+[Al(HL)(OH)(NO_3)(H_2O)]$ (calcd m/z 385.0453) and $Na^+[Al(HL)(OH)(NO_3)(H_2O)(DMSO)]$ (calcd m/z 463.0592), respectively. In Fig. 5b, the peak at m/z 394.0518 corresponds to the ion $[Zn(HL)(H_2O)(DMF)]^+$ (calcd m/z 394.7172), and m/z 450.1390 corresponds to the ion $K^+[Zn(HL)(OH)(H_2O)(DMF)]$ (calcd m/z 450.8400).

Dalton Transactions Accepted Manuscript

From Job plot, ^{1}HNMR data and ESI-MS results, it can be concluded that the Al^{3+} complex in DMSO and Zn^{2+} complex in DMF may be [Al(HL)(OH)(NO_3)(H_2O)(DMSO)] and [Zn(HL)(OH)(H_2O)(DMF)], respectively (Scheme 1). In fact, six-coordinated Al^{3+} complexes and five- coordinated Zn^{2+} complexes are commonly seen.[59-64]

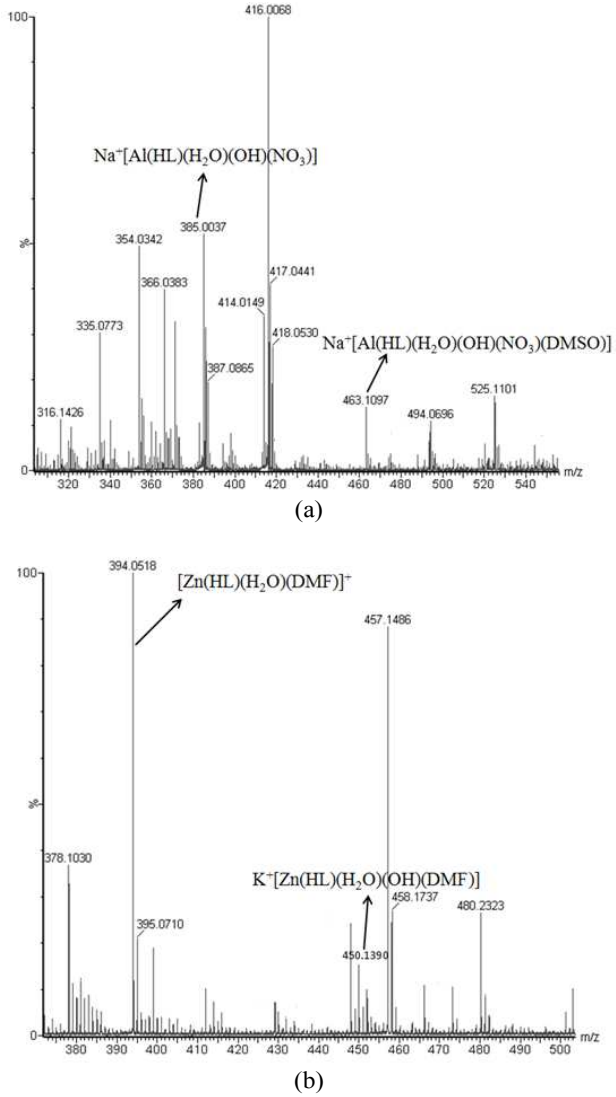

Fig. 5 ESI-MS spectrum of H_2L upon addition (a)1.0 equiv of Al^{3+}, (b)1.0 equiv of Zn^{2+}.

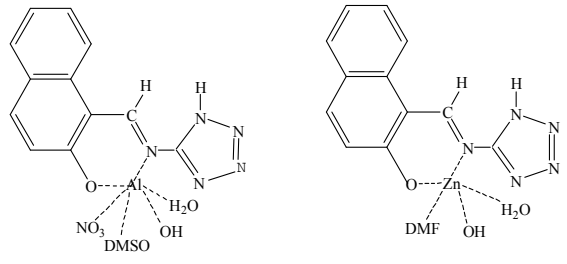

Scheme 1. The possible species of complexation of H_2L with (a) Al^{3+} in DMSO and (b) Zn^{2+} in DMF.

Theoretical calculations for sensing mechanism

In DMF and DMSO, H_2L exhibited weak fluorescence. To figure out whether ESIPT for H_2L would play an important role, theoretical calculations were carried out (Table S1). There are three possible isomers, i.e., S_0-a, S_0-b, and S_0-c in Fig. 6. Two

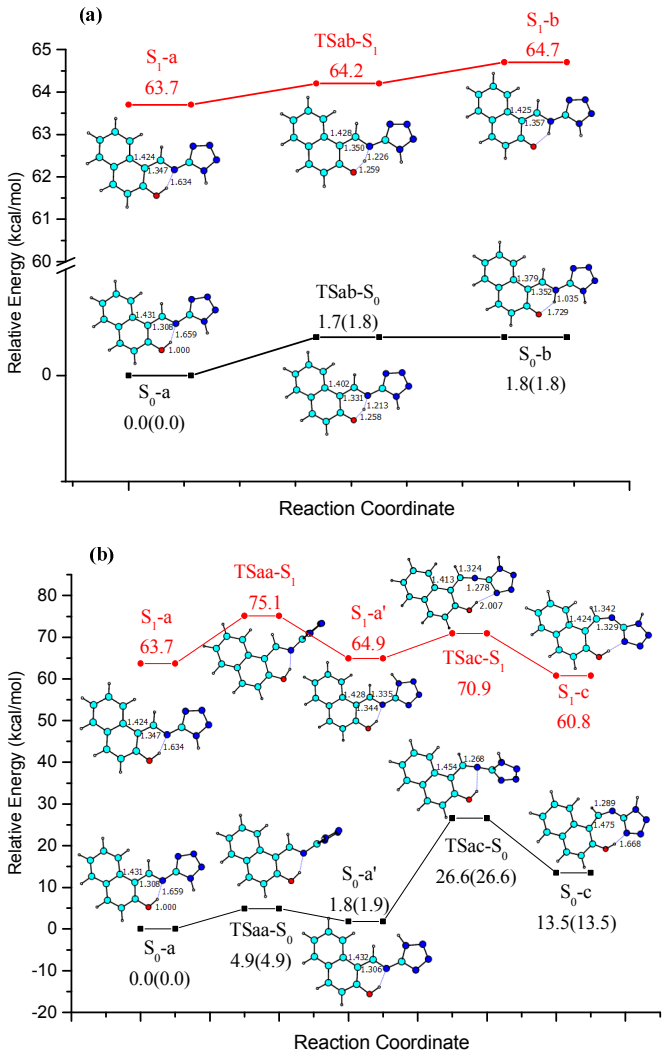

Fig. 6 The hydrogen transfer (a) and trans-cis isomerization (b) processes for H_2L in ground- and excited-state, along with key geometrical parameters (bond length in Angstrom and bond angel and dihedral angel in degree) and relative energies (in kcal/mol) in DMSO solvent at the level of B3LYP/6-311G** for ground state and TD-B3LYP/6-311G** for excited state. The data in parentheses are in DMF solvent.

possible reaction paths including hydrogen transfer between S_0-a and S_0-b, and imine isomerization between S_0-a and S_0-c have been considered, as depicted in Figure 6(a) and 6(b). In the ground state, hydrogen transfer from S_0-a to S_0-b is completed via TSab-S_0 with an energy demand of 1.8 kcal/mol in DMSO/DMF solvent. The reverse reaction is energy barrier free. In the excited state, only the calculations in DMSO solvent were carried out since the DMSO and DMF solvents have the

Dalton Transactions Accepted Manuscript

This journal is © The Royal Society of Chemistry 2012

similar effect on the ground-state stationary points. The results show that the hydrogen transfer can proceed very easily, just the same as in the ground state. For the imine isomerization from S_0-a to S_0-c isomers, the present calculations suggest a two-step mechanism, the intramolecular rotation around N6-C7 (the numbering system see Figure 4) bond via TSaa-S_0, and the followed flip-flap of C5-N6-C7 bond angle via TSac-S_0, which corresponds to a C5-N6 bond rotation. In the ground state, the second step is rate-determining with a relative energy of 26.6 kcal/mol in DMSO/DMF with respect to S_0-a, which is inaccessible in energy at room temperature. In the excited state, the first step is rate-determining with an energy barrier of 11.4 kcal/mol in DMSO solvent since the N6-C7 bond has more double bond character, which can not compete against hydrogen transfer between S_0-a and S_0-b.

Kinetically, the hydrogen transfer process is preferential both in the ground- and excited-state. Thermodynamically, the relative energies of S_0-b and S_0-c are 1.8/1.8 and 13.5/13.5 kcal/mol in DMSO/DMF solvent with respect to S_0-a. Obviously, H_2L is mainly in the form of S_0-a in equilibrium in the ground state. When promoted to excited state, however, the adiabatic excitation energies are 63.7(63.7-0.0), 62.9(64.7-1.8) and 47.3 (60.8-13.5) kcal/mol for S_1-a, S_1-b, and S_1-c, respectively. Even S_1-c is energetically favorable in excited state, S_1-a to S_1-c is kinetically hard to achieve because of the higher energy barrier for TSaa-S_1 and TSac-S_0.

The present calculations suggest that H_2L exists in the form of S_0-a in the ground state and S_1-a in the excited state, and hydrogen transfer takes place preferentially both in the ground- and excited-state, which is responsible for the weakness of the fluorescence of H_2L. Upon coordination with Al^{3+}/Zn^{2+}, this process for H_2L is inhibited, resulting in the large fluorescence enhancement.

Bioimaging studies of live cells

Having researched the excellent selectivity and high sensitivity of H_2L towards Al^{3+} ion in DMSO and Zn^{2+} ion in DMF, we further explored its potential application in living cell bioimaging. To achieve this, the human cervical HeLa cancer cells were first incubated separately with $Al(NO_3)_3$ and $Zn(NO_3)_2$ for 4 h and then treated with 10 μM H_2L for 30 min. As shown in Fig. 7, these cells that were not incubated with H_2L previously showed no fluorescence, while strong fluorescence was observed in cells exposed to H_2L. These results demonstrated that the chemosensor H_2L could be applied in imaging of intracellular Al^{3+} and Zn^{2+} ions.

Conclusions

A highly selective and sensitive tetrazole derivative-based fluorescence chemosensor H_2L for Al^{3+} ion in DMSO and Zn^{2+} ion in DMF was synthesized. The possible fluorescent species of H_2L with Al^{3+}/Zn^{2+} were deduced according to Job plot, ^{1}HNMR and ESI-MS. In addition, theoretical calculations explained the ESIPT sensing mechanism. What's more, the chemosensor H_2L could be used to detect intracellular Al^{3+} and Zn^{2+} ions. This design of nitrogen- and oxygen-rich small molecules can serve as a platform to explore fluorescent chemosensor for detection of multi-metal ions.

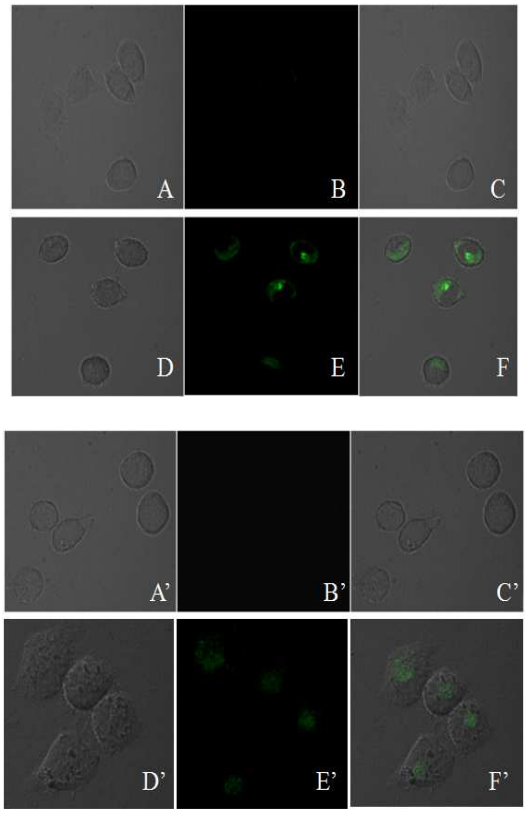

Fig. 7 Confocal fluorescence images of Al^{3+}(A, B, C, D, E, F) and Zn^{2+}(A', B', C', D', E', F') in human HeLa cells. The Bright-field (A, A'), fluorescent (B, B'), and overlay (C, C') images of Hela cells incubated with $Al(NO_3)_3/Zn(NO_3)_2$ for 4h. The Bright-field (D, D'), fluorescent (E, E'), and overlay (F, F') images of HeLa cells incubated with $Al(NO_3)_3/Zn(NO_3)_2$ for 4h and exposed to 10 μM H_2L for 30min. λ_{ex} = 405nm.

Experimental section

Material and Method

All chemicals were available commercially and used as received without further purification. Elemental analyses (CHN) were measured using a Vario EL elemental analyzer. Fluorescence spectra were conducted on a Varian Cary Eclipse fluorescence spectrophotometer equipped with a quartz cuvette of 1.0 cm path length with a xenon lamp as the excitation source. UV-Vis absorption spectra were determined on TU-1901 spectrophotometer. Fourier transform infrared (FT-IR) spectra were recorded on a Avatar 360 FI-IR spectrometer using KBr pellets in the range of 4000–400 cm^{-1}. ^{1}HNMR spectra were measured on a Bruker Avance III 400 MH_Z spectrometer in DMSO-d_6 and DMF-d_7 solution with TMS as an internal standard. ESI-MS spectra were obtained with an LCT Premier XE time-of-flight (TOF) mass spectrometer.

Dalton Transactions Accepted Manuscript

Synthesis of 1-[(1H-tetrazol-5-ylimino)methyl]naphthalen-2-ol (H_2L)

A mixture containing 2-hydroxy-1-naphthaldehyde (0.051g, 0.3mmol), 5-amino-1H-tetrazole (0.026g, 0.3mmol) and 3 mL methanol was sealed in a 25 mL Teflon-lined autoclave and heated at 80 °C for 24 h and then allowed to cool to room temperature. Yellow needle-like crystals of H2L were obtained in a yield of 66.3% after washed with methanol and air-dried. Anal. Calcd for $C_{12}H_9N_5O$: C, 60.25; N, 29.27; H, 3.79. Found: C, 60.21; N, 29.31; H, 3.64. IR (KBr pellet, cm^{-1}): 3438(m), 3016(m), 2488(m), 1811(m), 1608(s), 1556(s), 1410(m), 1307(s), 1174(m), 1052(m), 745(m). 1H NMR DMSO-d6, 400 MHz) δ (ppm): 13.35 (s, 1H), 10.12 (s, 1H), 8.78-8.80 (d, 1H J = 8.28 Hz), 8.13-8.15 (d, 1H J = 8.92 Hz), 7.92-7.94 (d, 1H J = 8.08 Hz), 7.64–7.67 (t, 1H J = 7.12 Hz), 7.45-7.48 (t, 1H J = 7.8 Hz), 7.26-7.28 (d, 1H J = 9.0 Hz). 1H NMR(DMF-d7, 400 MHz) δ (ppm): 14.12 (s, 1H), 10.50 (s, 1H), 8.85-8.87 (d, 1H J = 8.12 Hz), 8.38-8.41 (d, 1H J = 8.92 Hz), 8.16 (s, 1H), 7.87-7.91 (t, 1H J = 7.28 Hz), 7.67-7.70 (t, 1H J = 6.86 Hz), 7.47-7.49 (d, 1H J = 8.8 Hz).

Methods for living cells bioimaging

Human HeLa cells were cultured in DMEM (Dulbecco's modified Eagle's medium) supplemented with 10% fetal bovine serum (FBS) at 37 °C and saturated humidity in a incubator in the atmosphere of 95% air and 5% CO_2. Cells were seeded onto a 14 mm diameter glass at a density of 5×10^8 cells. Cells were then incubated with 10 μM of $Al(NO_3)_3$ and $Zn(NO_3)_2$ in PBS solution at 37°C for 4 h, respectively. After washing with PBS three times to remove the remaining $Al(NO_3)_3$ and $Zn(NO_3)_2$, the cells were then incubated with 10 μM of H_2L in DMSO (DMF)/PBS (1:99, v/v) solution for 30 min at room temperature. The incubated cells were washed with PBS and mounted onto a glass slide. Fluorescence images of the mounted cells were obtained using a confocal laser scanning microscope with 405 nm excitation.

Calculation methods

In this work, the B3LYP[65] functional of density functional theory(DFT) was employed using the Gaussian 09 program package[66]. All the ground-state stationary points reported here were fully optimized at the level of B3LYP/6-311G** and the excited-state ones at TD-B3LYP/6-311G**.[67,68] All the stationary points were confirmed to be a minimum or a transition state by frequency calculations. The effect of solvent has been considered using continuum solvation model SMD[69] with DMSO or DMF as solvent.

Acknowledgements

This work is supported by the National Natural Science Foundation of China (20971015 and 21073013), the Hong Kong Scholar Program and the Fundamental Research Funds for the Central Universities.

Notes and references

Beijing Key Laboratory of Energy Conversion and Storage Materials, College of Chemistry, Beijing Normal University, Beijing, 100875, People's Republic of China
E-mail: xjzheng@bnu.edu.cn(X.J. Zheng); Tel: 86-10-58805522

† Electronic Supplementary Information (ESI) available: Figures S1-S3 and Table S1 are provided in the Supporting Information. See DOI: 10.1039/b000000x/.

1 A. P. de Silva, H. Q. N. Gunaratne, T. Gunnlaugsson, A. J. M. Huxley, C. P. McCoy, J. T. Rademacher, T. E. Rice, *Chem. Rev*., 1997, **97**, 1515-1566.
2 J. Burgess, *Chem. Soc. Rev*., 1996, **25**, 85-92.
3 J. Barcelo, C. Poschenrieder, *Environ. Exp. Bot*., 2002, **48**, 75-92.
4 B. Wang, W. Xing, Y. Zhao, X. Deng, *Environ. Toxicol. Pharmacol*., 2010, **29**, 308–313.
5 E. Altschuler, *Med. Hypotheses*. ,1999, **53**, 22–23.
6 S. R. Powell, *J. Nutr*., 2000, **130**, 1447S-1454S;
7 T. M. Bray, W. J. Bettger, *Free Radical Biol. Med.*, 1990, **8**, 281-291.
8 J. M. Berg, Y. Shi, *Science*., 1996, **271**, 1081-1085.
9 X. M. Xie, T.G. Smart, *Nature*., 1991, **349**, 521-524.
10 A. P. de Silva, D. B. Fox, H. J. M. Huxley, T. S. Moody, *Coord. Chem. Rev*., **2000**, 205, 41-47.
11 M. M. Henary, Y. Wu, C. J. Fahrni, *Chem. Eur. J*., 2004, **10**, 3015-3025.
12 Z. C. Xu, K. H. Baek, H. N. Kim, J. N. Cui, X. H. Qian, D. R. Spring, I. Shin, J. Yoon, *J. Am. Chem. Soc*., 2010, **132**, 601-610.
13 A. Torrado, G. K. Walkup, B. Imperiali, *J. Am. Chem. Soc*., 1998, **120**, 609-610.
14 T. Jin, J. Lu, M. Nordberg, *Neuro. toxicology*., 1998, **19**, 529-536.
15 V. Bhalla, Roopa, M. Kumar, *Dalton Trans*., 2013, **42**, 975-980.
16 P. W. Du, S. J. Lippard, *Inorg. Chem*., 2010, 49, 10753-10755.
17 M. Arduini, P. Tecilla, *Chem. Commun*., 2003, **13**, 1606–1607.
18 J. S. Kim, J. Vicens, *Chem. Commun*., 2009**, 45,** 4791–4802.
19 S. Kim, J. Y. Noh, K. Y. Kim, J. H. Kim, H. K. Kang, S. W. Nam, S. H. Kim, S. Park, C. Kim, J. Kim, *Inorg. Chem*., 2012, **51**, 3597-3602.
20 S. H. Kim, H. S. Choi, J. Kim, S. J. Lee, D. T. Quang, J. S. Kim, *Org. Lett*., 2010, **12**, 560-563.
21 F. K. W. Hau, X. M. He, W. H. Lam, V. W. Yam, *Che ,m. Commun*., 2011, **47**, 8778-8780.
22 Y. Lu, S. S. Huang, Y. Y. Liu, S. He, L. C. Zhao, X. S. Zeng, *Org. Lett*., 2011, **13**, 5274-5277.
23 T. H. Ma, M. Dong, Y. M. Dong, Y. W. Wang, Y. Peng, *Chem.- Eur. J*., 2010, **16**, 10313-10318.
24 T. Y. Han, X. Feng, B. Tong, J. B. Shi, L. Chen, J. Q. Zhi, Y. P. Dong, *Chem. Commun*., 2012, **48**, 416-418.
25 W. H. Ding, W. Cao, X. J. Zheng, D. C. Fang, W. T. Wong, L. P. Jin, *Inorg. Chem*., 2013, **52**, 7320-7322.
26 E. M. Nolan, S. J. Lippard, *Acc. Chem. Res*., 2009, **42**, 193-203
27 V. Bhalla, H. Arora, A. Dhir, M. Kumar, *Chem. Commun*., 2012, **48**, 4722–4724.
28 K. Jobe, C. H. Brennan, M. Motevalli, S. M. Goldup, M. Watkinson, *Chem. Commun*., 2011, **47**, 6036–6038.
29 S. Huang, R. J. Clark, L. Zhu, *Org. Lett.*, 2007, **9**, 4999-5002.
30 S. C. Burdette, G. K. Walkup, B. Spingler, R. Y. Tsien, S.J. Lippard, *J. Am. Chem. Soc*., 2001, **123**, 7831-7841.
31 S. C. Burdette, C. J. Frederickson, W. Bu, S. J. Lippard. *J. Am. Chem. Soc*., 2003, **125**, 1778-1787.

Dalton Transactions Accepted Manuscript

 This journal is © The Royal Society of Chemistry 2012

32 K. Hanaoka, K. Kikuchi, H. Kojima, Y. Urano, T. Nagano, *J. Am. Chem. Soc*., 2004, **126**, 12470-12476.
33 A. Ajayaghosh, P. Carol, S. Sreejith. *J. Am. Chem. Soc*., 2005, **127**, 14962-14963.
34 K. Komatsu, Y. Urano, H. Kojima, T. Nagano. *J. Am. Chem. Soc*., 2007, **129**, 13447-13454.
35 F. Qian, C. L. Zhang, Y. M. Zhang, W. J. He, X. Gao, P. Hu, Z. J. Guo. *J. Am. Chem. Soc*., 2009, **131**, 1460-1468.
36 Z. C. Xu, K. H. Baek, H. N. Kim, J. N. Cui, X. H. Qian, D. R. Spring, I. Shin, J. Y. Yoon. *J. Am. Chem. Soc*., 2010, **132**, 601-610.
37 L. Xue, G. P. Li, C. L. Yu, H. Jiang. *Chem.- Eur. J*., 2012, **18**, 1050-1054.
38 D. Maity, T. Govindaraju. *Chem. Commun*., 2012, **48**, 1039-1041.
39 M. Shellaiah, Y. H. Wu, H. C. Lin. *Analyst*., 2013, **138**, 2931-2942.
40 V. Bavetsias, J. H. Marriott, C. Melin, R. Kimbell, Z. S. Ma-tusiak, F. T. Boyle, A. L. Jackman, *J. Med. Chem*., 2000, **43**, 1910–1926.
41 R. S. Upadhayaya, S. Jain, N. Sinha, N. Kishore, R. Chandra, S. K. Arora, *Eur. J. Med. Chem.*, 2004, **39**, 579–592.
42 V. A. Ostrovskii, R. E. Trifonov, E. A. Popova, *Russ. Chem. Bull*. 2012, **61**, 768–780.
43 R. N. Butler, in: Comprehen-sive Heterocyclic Chemistry, vol. 5, part 4.13 (Eds.: A. R. Ka-tritzky, C. W. Rees), *Elsevier Science, Ltd*. 1984, p. 791–838.
44 H. Gao, J. M. Shreeve, *Chem. Rev*., 2011, **111**, 7377–7436.
45 E. A. Popova, R. E. Trifonov, V. A. Ostrovskii, *ARCIVOC*., 2012, 45–65.
46 G. Aromí, L. A. Barrios, O. Roubeau, P. Ga-mez, *Coord. Chem. Rev*., 2011, **255**, 485–546
47 H. Torii, M. Naka-dai, K. Ishihara, S. Saito, H. Yamamoto, *Angew. Chem. Int. Ed*., 2004, **43**, 1983–1986.
48 K. R. Knudsen,C. E. T. Mitchell, S. V. Ley, *Chem. Commun*., 2006, 66–68.
49 Y. Yamamoto, N. Momiyama, H. Yamamoto, *J. Am. Chem. Soc*., 2004, **126**, 5962–5963.
50 O. I. Shmatova, V. G. Nenajdenko, *Eur. J. Org. Chem*., 2013, 6397–6403.
51 D. Maity, T. Govindaraju, *Inorg. Chem*., 2010, **49**, 7229–7231.
52 S. Huang, R.J. Clark, L. Zhu. *Org. Lett*., 2007, **9**, 4999-5002.
53 A. K. Mishra, N. Manav, N. K. Kaushik, *Spectrochim. Acta, Part A*., 2005, **61**, 3097-3101.
54 M. G. Wahed, E. M. Nour, S. Teleb, S. Fahim, J. Therm. *Anal. Calorim*., 2004, **76**, 343-348.
55 H. A. Benesi, J. H. Hildebrand, *J. Am. Chem. Soc.*, 1949, **71**, 2703-2707.
56 Y. Zhang, X. F. Guo, L. H. Jia, S. C. Xu, Z. H. Xu, L. B. Zheng, X. H. Qian, *Dalton Trans*., 2012, **41**, 11776-11782.
57 M. Shellaiah, Y. H. Wu, H. C. Lin, *Analyst*., 2013, **138**, 2931-2942.
58 E. Stavitski, M. Goesten, J. J. AlcaÇiz, A. M. Joaristi, P. S. Crespo, A. V. Petukhov, J. Gascon, F. Kapteijn, *Angew. Chem. Int. Ed*., 2011, **50**, 9624-9628.
59 H. Reinsch, B. Marszalek, J. Wack, J. Senker, B. Gil, N. Stock, *Chem. Commun*., 2012, **48**, 9486-9488.
60 H. Reinsch, M. A. van der Veen, B. Marszalek, T. Verbiest, D. de Vos, N. Stock, Chem. Mater., 2013, 25, 17-26.
61 W. H. Casey, *Chem. Rev*., 2006, **106**, 1-16.
62 T. Ahnfeldt, D. Gunzelmann, J. Wack, J. Senker, N. Stock, *CrystEngComm*., 2012, **14**, 4126-4136.
63 X. Y. Zhou, P. X. Li, Z. H. Shi, X. L. Tang, C. Y. Chen, W. S. Liu, *Inorg. Chem*., 2012, **51**, 9226-9231.
64 S. C. Burdette, G. K. Walkup, B. Spingler, R. Y. Tsien, S. J. Lippard, *J. Am. Chem. Soc*., 2001, **123**, 7831-7841.
65 A. D. Becke, *J. Chem. Phys.*, 1993, **98**, 5648-5652.
66 M. J. Frisch, G. W. Trucks, H. B. Schlegel, G. E. Scuseria, M. A. Robb, J. R. Cheeseman, G. Scalmani, V. Barone, B. Mennucci, G. A. Petersson, H. Nakatsuji, M. Caricato, X. Li, H. P. Hratchian, A. F. Izmaylov, J. Bloino, G. Zheng, J. L. Sonnenberg, M. Hada, M. Ehara, K. Toyota, R. Fukuda, J. Hasegawa, M. Ishida, T. Nakajima, Y. Honda, O. Kitao, H. Nakai, T. Vreven, J. A. Montgomery,; J. E. Jr., Peralta, F. Ogliaro, M. Bearpark, J. J. Heyd, E. Brothers, K. N. Kudin, V. N. Staroverov, T. Keith, R. Kobayashi, J. Normand, K. Raghavachari, A. Rendell, J. C. Burant, S. S. Iyengar, J. Tomasi, M. Cossi, N. Rega, J. M. Millam, M. Klene, J. E. Knox, J. B. Cross, V. Bakken, C. Adamo, J. Jaramillo, R. Gomperts, R. E. Stratmann, O. Yazyev, A. J. Austin, R. Cammi, C. Pomelli, J. W. Ochterski, R. L. Martin, K. Morokuma, V. G. Zakrzewski, G. A. Voth, P. Salvador, J. J. Dannenberg, S. Dapprich, A. D. Daniels, Ö. Farkas, J. B. Foresman, J. V. Ortiz, J. Cioslowski, D. J. Fox, Gaussian 09, Gaussian, Inc., Wallingford CT, 2010.
67 F. Furche, R. Ahlrichs, *J. Chem. Phys.*, 2002, **117**, 7433-7447.
68 G. Scalmani, M. J. Frisch, B. Mennucci, J. Tomasi, R. Cammi, V. Barone, *J. Chem. Phys.*, 2006, **124**, 094107:1-15.
69 A. V. Marenich, C. J. Cramer, D. G. Truhlar, *J. Phys. Chem. B* 2009, **113**, 6378–6396.

Dalton Transactions Accepted Manuscript